Original article
DOI: https://doi.org/10.18721/JPM.14401

OPTICAL-ELECTRIC PHASE CHARACTERISTICS OF SILICON NEGATIVE-U NANOSANDWICHES

N. I. Rul' [1,2]✉, *P. A. Golovin* [1,2], *N. T. Bagraev* [2,1], *L. E. Klyachkin* [2], *A. M. Malyarenko* [2]

[1] Peter the Great St. Petersburg Polytechnic University, St. Petersburg, Russia;

[2] Ioffe Institute of the Russian Academy of Sciences, St. Petersburg, Russia

✉ rul.nickolai@mail.ru

Abstract: In order to determine the possibility of the phase control of terahertz (THz) radiation from silicon negative-U nanosandwich structures (NSS), as well as to describe the relationship of optical and electrical characteristics of these NSS, the room-temperature measurement of modulated electroluminescence spectra have been carried out. In so doing, the opportunity to adjust a frequency, an amplitude and a phase of THz radiation was found; the longitudinal conductance phase characteristics of the edge channels of the NSS were recorded at high temperature (up to room one). The physical processes underlying the observed phenomena were analyzed. The edge channels' cooling effect as a contributory factor for observation of the high-temperature macroscopic quantum phenomena arised due to the strong exchange interaction between the charge carriers in the edge channels and the dipole boron centers with negative correlation energy (negative-U reaction). The explanation of the observed phenomena using the quantum Faraday effect made it possible to apply the NSS as a component base for the silicon radiophotonics.

Keywords: silicon nanosandwich, negative correlation energy, dipole boron centers, terahertz radiation

Funding: The reported study was funded by RFBR according to the research project No. 20-32-90130 "The quantum spin Faraday effect in the low-dimensional silicon negative-U nanosandwich-structures at high temperatures".

Citation: Rul' N. I., Golovin P. A., Bagraev N. T., Klyachkin L. E., Malyarenko A. M., Optical-electric phase characteristics of silicon negative-U nanosandwiches, St. Petersburg Polytechnical State University Journal. Physics and Mathematics. 14 (4) (2021) ...–... . DOI: 10.18721/JPM.14401

Научная статья
УДК
DOI: https://doi.org/10.18721/JPM.14401

ОПТИКО-ЭЛЕКТРИЧЕСКИЕ ФАЗОВЫЕ ХАРАКТЕРИСТИКИ КРЕМНИЕВЫХ НАНОСАНДВИЧЕЙ С ОТРИЦАТЕЛЬНОЙ КОРРЕЛЯЦИОННОЙ ЭНЕРГИЕЙ

Н. И. Руль [1,2] ✉, *П. А. Головин* [1,2], *Н. Т. Баграев* [2,1],
Л. Е. Клячкин [2], *А. М. Маляренко* [2]

[1] Санкт-Петербургский политехнический университет Петра Великого, Санкт-Петербург, Россия;

[2] Физико-технический институт им. А.Ф. Иоффе РАН, Санкт-Петербург, Россия

✉ rul.nickolai@mail.ru

Аннотация. С целью выявления возможности фазового контроля терагерцового (ТГц) излучения из кремниевых наносандвич-структур, а также описания взаимосвязи оптических и электрических характеристик подобных наноструктур, в работе проведены измерения спектров модулированной электролюминесценции указанных структур при комнатной температуре. При этом установлена возможность корректировки частоты, амплитуды и фазы ТГц-излучения; зарегистрированы фазовые характеристики продольной проводимости краевых каналов кремниевых negative-U-наносандвичей при высокой температуре (вплоть до комнатной). Проанализированы физические процессы, лежащие в основе наблюдаемых явлений. Эффект охлаждения краевых каналов, способствующий наблюдению высокотемпературных макроскопических квантовых явлений, возникает благодаря наличию сильного обменного взаимодействия между носителями тока в краевых каналах и дипольными центрами бора с отрицательной корреляционной энергией (negative-U-реакция). Объяснение наблюдаемых явлений с помощью квантового эффекта Фарадея подтверждает возможность использования представляемых наноструктур в качестве компонентной базы для кремниевой радиофотоники.

Ключевые слова: кремниевый наносандвич, отрицательная корреляционная энергия, дипольный центр бора, терагерцовое излучение

Финансирование: Исследование выполнено при финансовой поддержке РФФИ в рамках научного проекта № 90130-32-20 «Квантовый спиновый эффект Фарадея в низкоразмерных кремниевых negative-U наносандвич-структурах при высоких температурах».

Для цитирования: Руль Н. И., Головин П. А., Баграев Н. Т., Клячкин Л. Е., Маляренко А. М. Оптико-электрические фазовые характеристики кремниевых наносандвичей с отрицательной корреляционной энергией // Научно-технические ведомости СПбГПУ. Физико-математические науки. 2021. Т. 14. № 4. С. 9–20. DOI: 10.18721/JPM.14401

Introduction

Constructing portable and tunable sources and recorders for far infrared (FIR) and terahertz (THz) ranges of electromagnetic radiation [2, 6–11] is one of the fundamental unsolved problems of modern optics. Nevertheless, silicon nanosandwiches prepared within Hall geometry (Fig. 1,*a*) [1] confirm that it is possible to transmit and record terahertz radiation by generating topological edge channels (Fig. 1,*b*,*d*) confined by trigonal dipole boron centers $2B^0 \rightarrow B^- + B^+$ with negative correlation energy (negative-U) [1, 2] (Fig. 1,*c*). The complex energy spectrum of current carriers in the edge channels of silicon nanosandwiches, as well as suppression of thermal transitions compared to optical ones due to the cooling effect lead to observable amplitude and frequency-modulated THz electroluminescence. Amplitude and frequency THz modulation of infrared radiation is extremely important for it to effectively penetrate living matter. The potential of the given nanostructures for applications in radio-frequency silicon photonics heavily depends on whether such modulation of IR radiation is possible.

Thus, the goal of this study consisted in exploring the options for amplitude and frequency THz modulation and phase control of the radiation emitted from negative-U silicon nanosandwiches, describing the relationship between the optical and electrical characteristics of similar nanostructures.

In view of our goal, we considered the relationship of the characteristics of the radiation emitted from the given nanostructures with the transmitted drain-source current and the voltage applied to the external lateral and top gates.

Negative-U silicon nanosandwich structure

The silicon nanosandwich (SNS) considered in this study is an ultra-narrow *p*-type silicon quantum well (*p*-Si-QW), confined by delta barriers (Si:B) heavily doped with boron (boron concentration $N(\mathrm{B}) = 5 \cdot 10^{21}$ cm^{-3}), obtained on the surface of single-crystal *n*-type silicon (*n*-Si (100)) (Fig. 1,*a*). The SNS is made within Hall geometry by preliminary oxidation of silicon and subsequent rapid diffusion of boron from the gas phase [2]. It was found that a consequence of high boron concentration inside δ-barriers is that boron atoms inside such barriers are arranged in crystallographically oriented sequences of trigonal dipole centers $B^- + B^+$ produced through a negative-U $2B^0 \rightarrow B^- + B^+$ reaction [1, 2]. The two-dimensional carrier density in Si-QW is $n_{2D} = 3 \cdot 10^{13}$ m^{-2}. The model shows lateral (V_{lg}) and top (V_{tg}) gates, along with the longitudinal contacts U_{xx} (see Fig. 1,*a*). The model of the edge channel in a silicon nanosandwich (Fig. 1,*b* shows single current carriers (holes) confined by crystallographically oriented dipole centers. The trigonal dipole center of boron (Fig. 1,*c*) is a virtual Josephson junction with a superconducting correlation gap of $2\Delta = 44$ meV (10.64 THz). The model of carrier transport in the edge channel (Fig. 1,*d*) exhibits the quasi-one-dimensional sequences of boron dipole centers, confining the edge channels in SNS, and two back-to-back Josephson junctions at the interface between adjacent charge carriers in the channel.

Apparently, the presence of trigonal dipole boron centers greatly contributes to reducing the electron-electron interaction between charge carriers, consequently allowing to observe macroscopic quantum phenomena at high (up to room) temperatures [1]. Moreover, the most effective suppression of electron-electron interaction is achieved inside the edge channels of the silicon quantum well, confined by negative-U dipole centers. Notably, the magnitude of the negative correlation energy depends on the degree to which the electron-electron interaction is neutralized by the electron-vibrational interaction due to the presence of a local phonon mode [2]. Detailed analysis of the temperature dependences of conductance for crystallographically orientated edge channels in SNS yielded the negative-U magnitude of 0.044 eV [2], suggesting that macroscopic quantum phenomena can be observed at high temperatures.

Using planar silicon nanotechnology to prepare such quantum-sized *p*–*n*-junctions can produce a system of fractal microcavities embedded into the junction plane. A system of microcavities tuned to the frequencies characteristic for the IR range of electromagnetic waves makes it possible to enhance their radiation intensity. Besides, the boron doping nanotechnology allowing to produce delta barriers confining ultra-narrow silicon quantum wells has been thoroughly tested, so these structures can be used as generators of electromagnetic radiation in the terahertz (THz) and gigahertz (GHz) ranges [2]. The depth of THz modulation can be significantly increased by varying the distribution of the electric field in the edge channel with voltages applied to the lateral and top contacts acting as gates (similar to an optical transistor).

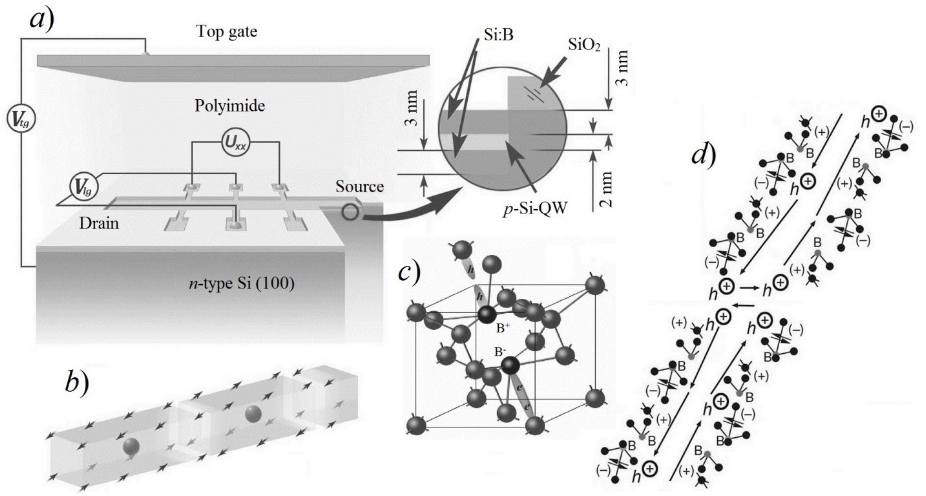

Fig. 1. Schematic model of the *p*-Si-QW (*a*) structure, its elements (*b*, *c*, inset in *a*) and carrier transport in the edge channel (*d*):
Si:B are the δ-barriers heavily doped with boron; *n*-Si (100) is the surface of *n*-type silicon; V_{lg}, V_{tg} are the voltages across the lateral and top gates, respectively; U_{xx} is the voltage across the longitudinal measuring contacts; *b* is the model of the edge channel in a silicon nanosandwich (black balls correspond to holes), *c* is the trigonal dipole boron center

Due to effective reduction of electron-electron interaction, the holes inside the edge channels form chains of quantum harmonic oscillators emitting THz and GHz radiation within the quantum Faraday effect provided that a stabilized drain-source current inducing a magnetic field is passed through the edge channels in the SNS. In turn, the magnetic flux quanta emerging during this process (h/e for single holes in normal chains of dipole centers and $h/2e$ for superconducting chains, when the segments of edge channels (called pixels) combine to produce pairs of holes, are 'captured' on the edge channels (see Fig. 1,*b*)), consequently creaing induced current leading to THz and GHz generation through the quantum Faraday effect:

$$I_{ind} \cdot \Delta\Phi = E(h\nu),$$

where $\Delta\Phi = \Phi_0 = h/e(h/2e)$.

Terahertz radiation can be generated by one of the two mechanisms, depending on the magnitude of the drain-source current [2].

We should note that the quantum Faraday effect is understood here as the quantum equivalent of the expression obtained by Laughlin [3, 4] to describe the quantum transport of particles in an external magnetic field, which has nothing in common with the magneto-optical Faraday effect. The key features of this approach are that an external magnetic field is absent, while the particle energy can be varied not only due to the potential difference applied to the lateral gates but also using the energy of electromagnetic quanta. In other words, the version of Laughlin's expression that we follow in this study is the quantum equivalent of the law of electromagnetic induction for the case when the variation in the magnetic flux induced by the passing current corresponds to a specific number of magnetic flux quanta captured per area of the given negative-U silicon nanostructures [1].

The mechanism described above, associated with the induced current I_{ind} (in pixels) generated as single magnetic flux quanta are captured, is predominant at low currents (below $9 \cdot 10^{-7}$ A). Generation of terahertz radiation for currents significantly exceeding this value is similar to that in a system with two back-to-back Josephson junctions (Fig. 1,*d*). In this case, the generation frequency is determined by the well-known expression:

$$h\nu = neI_{ind}R_0,$$

where R_0 is the resistance quantum for a single hole (or a pair of holes); $R_0 = h/e^2$ ($n = 1$) for a single hole, while $R_0 = h/4e^2$ ($n = 2$) for a pair of holes in superconducting chains of dipole centers.

Given that the two-dimensional density of current carriers in the quantum well in SNS is $n_{2D} = 3\cdot10^{13}$ m^{-2}, the dimensions of the pixel with a single hole are equal to 16.6 μm and 2.0 nm in the longitudinal and transverse directions, respectively, which, in turn, leads to predominant generation at 2.8 THz [2].

Phase control of THz-modulated electroluminescence

An external DC voltage applied to the *p*–*n* junction produces spin-orbit splitting of carrier energy under a drain-source current flowing in the edge channels [2]. The topological and superconducting properties of the edge channels in SNS were confirmed by observing and analyzing numerous macroscopic quantum effects, including the fractional quantum staircase of hole conductance in edge channels, the quantum Hall effect (including the quantum spin Hall effect), Shubnikov–de Haas and de Haas–van Alphen oscillations [1], as well as multiple Andreev reflection [1], respectively. Moreover, the reduction of electron-electron interaction between current carriers in the edge channels due to the negative-U reaction provides a cooling effect appearing as a dependence of the redshift in radiation on the transmitted current [1] due to strong exchange interaction of carriers with negative-U dipole boron centers. It is the presence of this effect that made it possible to observe THz electroluminescence at high temperatures (up to room temperature).

A Bruker IFS 115 spectrometer was used to measure modulated electroluminescence at room temperature ($T = 300$ K) (Figs. 2 and 3).

The modulated electroluminescence spectrum confirming that phase control is possible turns out to depend on both the transmitted current (Fig. 3) and the voltages applied to the top (V_{tg}) (Fig. 2, *e*–*g*) and lateral (V_{lg}) (Fig. 2, *a*–*c*) gates. The likely reason why the given THz radiation spectra appear is the presence of two back-to-back Josephson junctions inside the edge channel (nonstationary Josephson effect): these junctions emerge at the boundaries of neighboring pixels containing single holes (see Fig. 1,*d*). The junctions are described within the quantum Faraday effect provided that dissipation processes due to strong neutralization of electron-electron interaction. As long as the stabilized drain-source current I_{ds} remains below a certain critical value $I_{cr} \approx e/\tau$, where τ is the phase relaxation time of each single carrier, the electron-electron interaction is considerably reduced. However, when $I_{ds} > I_{cr}$ and the so-called overcritical current regime is established, the optical spectrum exhibits THz electroluminescence, depending on the magnitude of the current.

Because the edge channels are symmetric with respect to the top and lateral gates, the voltage applied to any gate acts (due to the above-mentioned quantum Faraday effect) as a compensating mechanism similar to the voltage applied to the virtual nonstationary Josephson junction. Applying a controlled voltage across such a double back-to-back Josephson junction, which is a boron dipole center with a negative correlation energy $2\Delta = 44$ meV [2] and a corresponding frequency of 10.64 THz, allows phase-controlling the spectral characteristics of THz radiation.

Fractional quantization of conductance

The electrical characteristics of SNS are related to the optical spectra presented above. The current-voltage characteristics of the edge channels in silicon nanosandwich structures exhibit fractional quantization of longitudinal conductance. The latter depends both on the magnitude of the transmitted stabilized drain-source current (as a quantization parameter) and on the voltage across the lateral gate (as a control parameter) applied to the Hall contacts (Fig. 4).

Significant decrease in the effective mass of current carriers [1] to $m^* \approx 2\cdot10^{-5}m_e$, together with reduction of electron-electron interaction between the carriers in the edge channels, in the subcritical current regime $I_{ds} < I_{cr}$ (I_{cr} is the critical current), provides a spin-dependent diamagnetic response of magnetic susceptibility (Fig. 5) depending on the strength of the external magnetic field [1]. Thus, the magnetic field induced by passing a drain-source current through a system of non-interacting carriers in turn generates diamagnetic or, in other words, induced current I_{ind}, which does not participate in charge transfer but can affect the magnitude of longitudinal conductance in the presence of a voltage across the lateral gate due to the quantum Faraday effect. Significant reduction in electron-electron interaction ultimately causes composite particles to appear by capturing single magnetic flux quanta into the system of non-interacting current carriers in the edge channels.

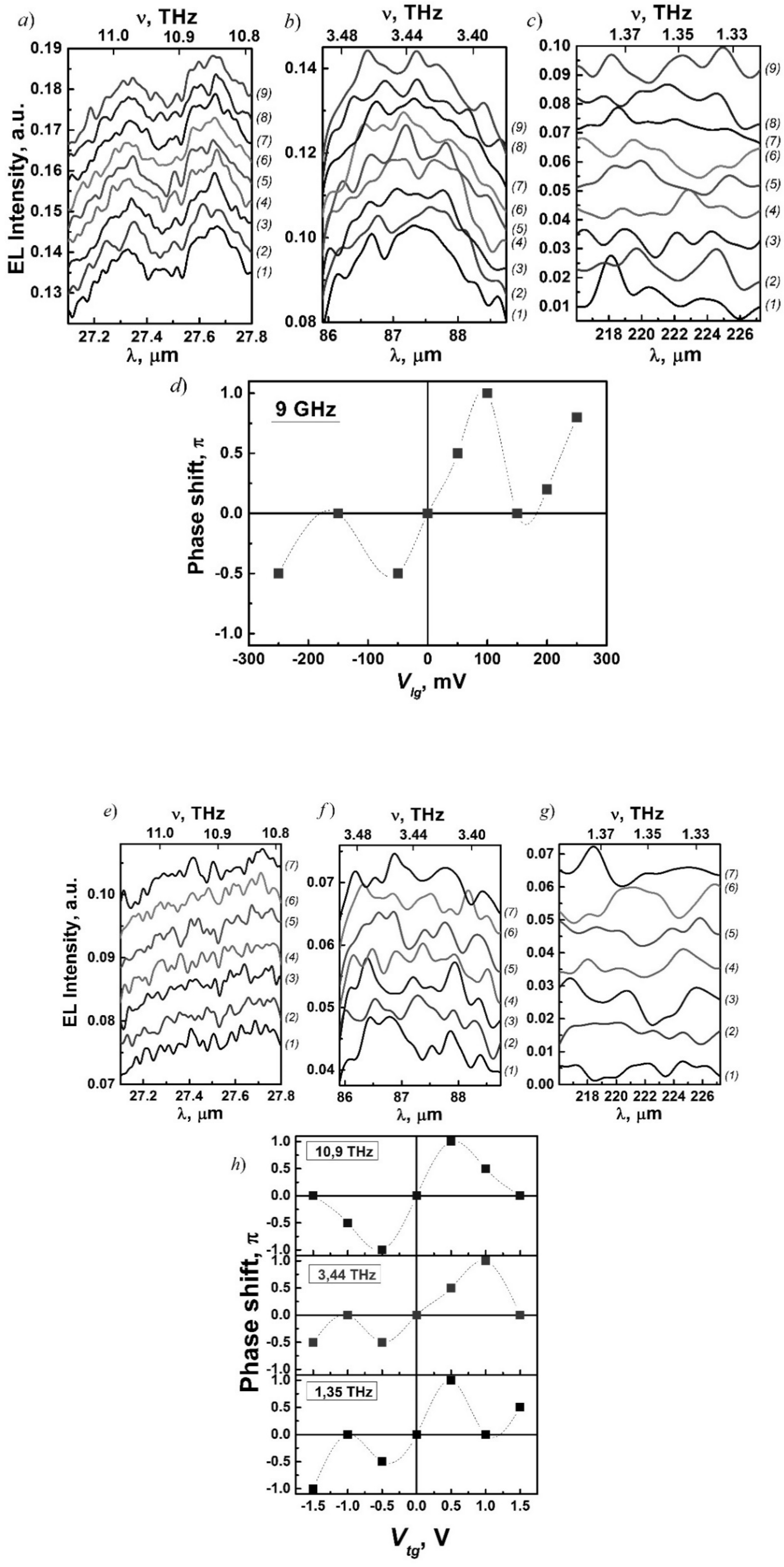

Fig. 2. THz-modulated electroluminescence spectra over three frequency ranges for different voltages across the lateral (V_{lg}, *a*–*c*) and top (V_{tg}, *e*–*g*) gates; phase shift as a function of these voltages V_{lg} (*d*) and V_{tg} (*h*). T = 300 K
V_{lg}, mV: −250 (*1*), −150 (*2*), −50 (*3*), 0 (*4*), 50 (*5*), 100 (*6*), 150 (*7*), 200 (*8*), 250 (*9*) (*a-c*);
V_{tg}, V: −1.5 (*10*), −1.0 (*11*), −0.5 (*12*), 0.0 (*13*), 0.5 (*14*), 1.0 (*15*), 1.49 (*16*).
Modulation frequency, THz: $9 \cdot 10^{-3}$ (*a*–*d*), 1.35 (*e*, *h*), 3.44 (*f*, *h*) and 10. 9 (*g*, *h*)

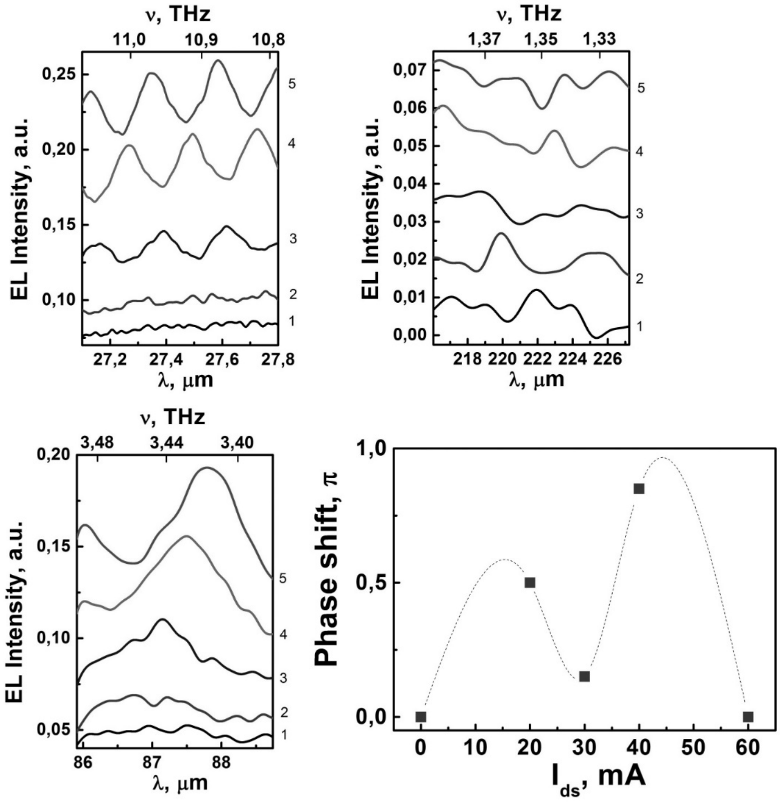

Fig. 3. THz-modulated electroluminescence spectra over three frequency ranges for different drain-source currents I_{ds} (*a*–*c*); phase shift as a function of this current (*d*). T = 300 K I_{ds}, mA: 0 (*1*), 20 (*2*), 30 (*3*), 40 (*4*) and 60 (*5*). Modulation frequency is 10.9 THz

This process is described by the Laughlin model [1, 3–5]:

$$I_{ind} = eV_{lg} / \Delta\Phi_V,$$

where $\Delta\Phi_V$ is the so-called gate phase, corresponding to the number of captured magnetic flux quanta $\Delta\Phi_V = eV_{lg}/I_{ind}$.

Phase control of the longitudinal conductance magnitude can be carried out by varying the voltage across the lateral Hall gate (see Fig. 4):

$$\Delta G = \Delta G_0\left(I_{ds}\right)\cdot\cos^2\left(\pi\frac{\Delta\Phi_I}{\Phi_0}+\varphi_I\right)\cos^2\left(\pi\frac{\Delta\Phi_V}{\Phi_0}+\varphi_V\right). \quad (1)$$

Here $\Delta\Phi_I$ is the current phase determining the number of magnetic flux quanta captured due to the self-induction phenomenon described by the well-known law $\Delta\Phi_I = L\cdot I_{ds}$; L, H, is the inductance of the edge channel.

Inductance depends on the magnitude of the drain-source current in a complex manner: $L(I_{ds})$. Analysis of this dependence requires further study, which is beyond the scope of this paper. However, the order of magnitude for inductance can be estimated from the given experiment, as well as through measuring the field dependences of static magnetic susceptibility [1]; it amounts to $(0.80–0.95)\cdot 10^{-4}$ H.

The difference in the values of the generated (induced) current I_{ds} in the range from 0.155 nA (see Fig. 4,*a*,*b*) to 1.356 nA (see Fig. 4,*c*) can be explained by scalability of the conductance maps presented for the negative-U silicon nanosandwich structure (see Fig. 4).

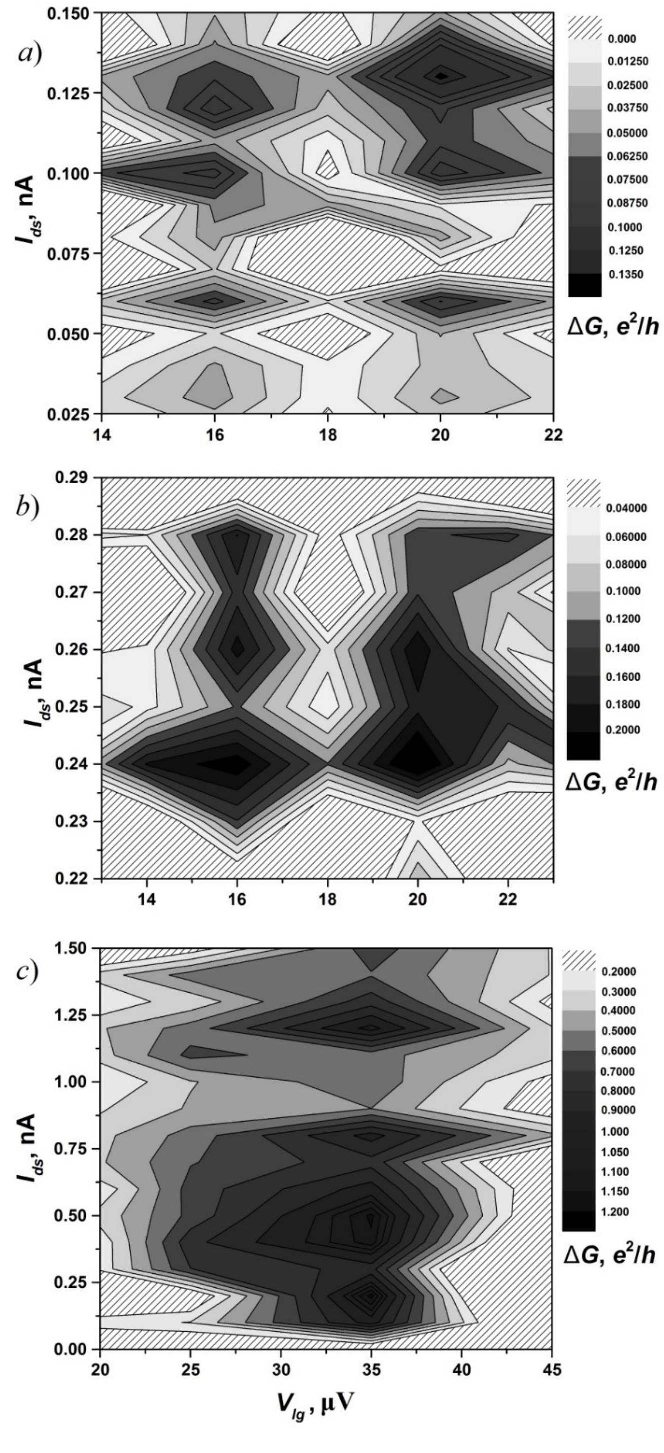

Fig. 4. Fractional quantum longitudinal conductance of edge channels in silicon nanosandwiches. Images *a*), *b*) and *c*) correspond to different steps in the sweep of the transmitted current and voltage across the lateral gate; $T = 300$ K.
The phase shift is determined by the number of magnetic flux quanta $\Delta\Phi_V$ and $\Delta\Phi_I$ captured into the edge channel

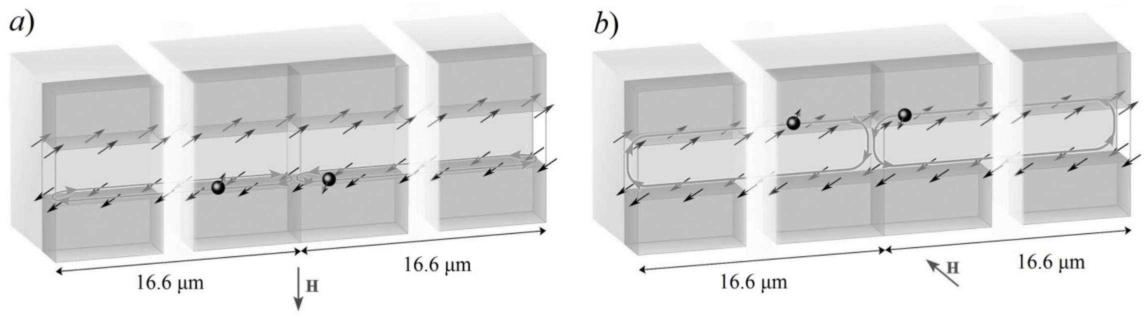

Fig. 5. Model of carrier transport in edge channels in the presence of vertical (*a*) and horizontal (*b*) external magnetic field

Notably, the experimental geometry was the same for obtaining the dependences of optical spectra on the magnitudes of the currents and gate voltages, and for measuring longitudinal conductance. The only difference was observed in the experiments with the nonstationary and stationary Josephson effect. Phase shifts in optical and electrical measurements have essentially the same nature and can be interpreted as a manifestation of the quantum Faraday effect. This means that single magnetic flux quanta are captured in the edge channel of the negative-U silicon nanosandwich, which occurs at room temperature.

Conclusion

The spectra obtained exhibit THz-modulated electroluminescence depending on the drain-source current and voltages across the lateral and top gates, and the options for phase control. The spectral characteristics of electroluminescence correspond to the phase characteristics of longitudinal conductance in the edge channels of a silicon quantum nanosandwich, confirming that these characteristics can be described simultaneously using the quantum Faraday effect.

Thus, phase inverters and optical modulators, as well as portable and tunable sources and recorders of terahertz radiation based on silicon nanosandwiches with such adjustable parameters as frequency, amplitude, and phase show potential for applications in terahertz silicon RF photonics.

Acknowledgment

N.I. Rul and P.A. Golovin express their gratitude to the Innovation Promotion Fund, UMNIK-20, for supporting the study *Design of a THz emitter for treatment of neurodegenerative diseases*, No. 0067237; to the Innovation Promotion Fund, UMNIK-19, for supporting the study *Design of spin silicon transistors for quantum computing at room temperature*, No. 0059806.

REFERENCES

1. **Bagraev N. T., Grigoryev V. Yu., Klyachkin L. E., et al.,** High-temperature quantum kinetic effect in silicon nanosandwiches, Low Temperature Physics. 43 (1) (2017) 110–119.

2. **Bagraev N. T., Golovin P. A., Khromov V. S., et al.,** Terahertz emitters based on negative-U materials for medical applications, Materials Physics and Mechanics. 44 (2) (2020) 264–270.

3. **Laughlin R. B.,** Quantized Hall conductivity in two dimensions, Phys. Rev. B. 23 (10) (1981) 5632–5633.

4. **Laughlin R. B.,** Anomalous quantum Hall effect: An incompressible quantum fluid with fractionally charged excitations, Phys. Rev. B. 50 (18) (1983) 1395–1398.

5. **Halperin B. I.,** Theory of the quantized Hall conductance, Helv. Phys. Acta. 56 (1–3) (1983) 75–102.

6. **Melentev G. A., Shalygin V. A., Vorobjev L. E., et al.,** Interaction of surface plasmon polaritons in heavily doped GaN microstructures with terahertz radiation, J. Appl. Phys. 119 (9) (2016) 093104.

7. **Vasilyev Yu. B., Mikhailov N. N., Vasilyeva G. Yu., et al.,** Terahertz emission from CdHgTe/HgTe quantum wells with an inverted band structure, Semiconductors. 50 (7) (2016) 915–919.

8. **Galimov A. I., Shalygin V. A., Moldavskaya M. D., et al.,** Optical properties of GaN/AlGaN nanostructures in the terahertz frequency range, J. Phys. Conf. Ser. 816 (1) (2017) 012019.

9. **Makhov I. S., Panevin V. Yu., Firsov D. A., et al.,** Impurity-assisted terahertz photoluminescence in quantum wells under conditions of interband stimulated emission, J. Phys. Conf. Ser. 993 (1) (2018) 012017.

10. **Shalygin V. A., Moldavskaya M. D., Panevin V. Yu., et al.,** Interaction of surface plasmon-phonon polaritons with terahertz radiation in heavily doped GaAs epilayers, J. Phys. Condens. Matter. 31 (10) (2018) 105002.

11. **Gorbenko I. V., Kachorovsky V. Yu., Shur M. S.,** Plasmonic polarization-sensitive detector of terahertz radiation, J. Phys. Conf. Ser. 1236 (1) (2019) 012029.

СПИСОК ЛИТЕРАТУРЫ

1. **Bagraev N. T., Grigoryev V. Yu., Klyachkin L. E., Malyarenko A. M., Mashkov V. A., Romanov V. V., Rul' N. I.** High-temperature quantum kinetic effect in silicon nanosandwiches // Low Temperature Physics. 2017. Vol. 43. No. 1. Pp. 110–119.

2. **Bagraev N. T., Golovin P. A., Khromov V. S., Klyachkin L. E., Malyarenko A. M., Mashkov V. A., Novikov B. A., Presnukhina A. P., Reukov A. S., Taranets K. B.** Terahertz emitters based on negative-U materials for medical applications // Materials Physics and Mechanics. 2020. Vol. 44. No. 2. Pp. 264–270.

3. **Laughlin R. B.** Quantized Hall conductivity in two dimensions // Physical Review B. 1981. Vol. 23. No. 10. Pp. 5632–5633.

4. **Laughlin R. B.** Anomalous quantum Hall effect: An incompressible quantum fluid with fractionally charged excitations // Physical Review B. 1983. Vol. 50. No. 18. Pp. 1395–1398.

5. **Halperin B. I.** Theory of the quantized Hall conductance // Helvetica Physica Acta. 1983. Vol. 56. No. 1–3. Pp. 75–102.

6. **Melentev G. A., Shalygin V. A., Vorobjev L. E., et al.** Interaction of surface plasmon polaritons in heavily doped GaN microstructures with terahertz radiation // Journal of Applied Physics. 2016. Vol. 119. No. 9. P. 093104.

7. **Васильев Ю. В., Михайлов Н. Н., Васильева Г. Ю. и др.** Терагерцовое излучение из квантовых ям CdHgTe/HgTe с инвертированной структурой зон // Физика и техника полупроводников. 2016. Т. 50. № 7. С. 932– 936.

8. **Galimov A. I., Shalygin V. A., Moldavskaya M. D., et al.** Optical properties of GaN/AlGaN nanostructures in the terahertz frequency range // Journal of Physics: Conference Series. 2017. Vol. 816. No. 1. P. 012019.

9. **Makhov I. S., Panevin V. Yu., Firsov D. A., Vorobjev L. E., Sofronov A. N., Vinnichenko M. Ya., Maleev N. A., Vasil'ev A. P.** Impurity-assisted terahertz photoluminescence in quantum wells under conditions of interband stimulated emission // Journal of Physics: Conference Series. 2018. Vol. 993. No. 1. P. 012017.

10. **Shalygin V. A., Moldavskaya M. D., Panevin V. Yu., et al.** Interaction of surface plasmon-phonon polaritons with terahertz radiation in heavily doped GaAs epilayers // Journal of Physics: Condensed Matter. 2018. Vol. 31. No. 10. P. 105002.

11. **Gorbenko I. V., Kachorovsky V. Yu., Shur M. S.** Plasmonic polarization-sensitive detector of terahertz radiation // Journal of Physics: Conference Series. 2019. Vol. 1236. No. 1. P. 012029.

THE AUTHORS

RUL' Nikolai I.
Peter the Great St. Petersburg Polytechnic University
Ioffe Institute of the Russian Academy of Sciences
29 Politechnicheskaya St., St. Petersburg, 195251, Russia
rul.nickolai@mail.ru
ORCID: 0000-0001-8991-6784

GOLOVIN Pavel A.
Peter the Great St. Petersburg Polytechnic University
Ioffe Institute of the Russian Academy of Sciences
29 Politechnicheskaya St., St. Petersburg, 195251, Russia
yellowcat0101@gmail.com
ORCID: 0000-0003-2876-2333

BAGRAEV Nikolay T.
Ioffe Institute of the Russian Academy of Sciences
Peter the Great St. Petersburg Polytechnic University
26 Polytekhnicheskaya St., St. Petersburg, 194021, Russia
bagraev@mail.ioffe.ru
ORCID: 0000-0001-8286-3472

KLYACHKIN Leonid E.
Ioffe Institute of the Russian Academy of Sciences
26 Polytekhnicheskaya St., St. Petersburg, 194021, Russia
klyachkin@mail.ioffe.ru
ORCID: 0000-0001-7577-1262

MALYARENKO Anna M.
Ioffe Institute of the Russian Academy of Sciences
26 Polytekhnicheskaya St., St. Petersburg, 194021, Russia
annamalyarenko@mail.ru
ORCID: 0000-0002-4667-7004

СВЕДЕНИЯ ОБ АВТОРАХ

РУЛЬ Николай Игоревич – *ассистент кафедры физики Санкт-Петербургского политехнического университета Петра Великого, младший научный сотрудник Физико-технического института им. А. Ф. Иоффе РАН.*
195251, Россия, г. Санкт-Петербург, Политехническая ул., 29
rul.nickolai@mail.ru
ORCID: 0000-0001-8991-6784

ГОЛОВИН Павел Александрович – *аспирант кафедры физики Санкт-Петербургского политехнического университета Петра Великого, младший научный сотрудник Физико-технического института им. А. Ф. Иоффе РАН.*
195251, Россия, г. Санкт-Петербург, Политехническая ул., 29
yellowcat0101@gmail.com
ORCID: 0000-0003-2876-2333

БАГРАЕВ Николай Таймуразович – *доктор физико-математических наук, ведущий научный сотрудник Физико-технического института им. А. Ф. Иоффе РАН, профессор кафедры физики Санкт-Петербургского политехнического университета Петра Великого.*
194021, г. Санкт-Петербург, Политехническая ул., 26
bagraev@mail.ioffe.ru
ORCID: 0000-0001-8286-3472

КЛЯЧКИН Леонид Ефимович – *кандидат физико-математических наук, старший научный сотрудник Физико-технического института им. А. Ф. Иоффе РАН.*
194021, г. Санкт-Петербург, Политехническая ул., 26
klyachkin@mail.ioffe.ru
ORCID: 0000-0001-7577-1262

МАЛЯРЕНКО Анна Михайловна – *научный сотрудник Физико-технического института им. А. Ф. Иоффе РАН.*
194021, г. Санкт-Петербург, Политехническая ул., 26
annamalyarenko@mail.ru
ORCID: 0000-0002-4667-7004

Received 16.11.2021. Approved after reviewing 22.11.2021. Accepted 22.11.2021.
Статья поступила в редакцию 16.11.2021. Одобрена после рецензирования 22.11.2021. Принята 22.11.2021.